RESEARCH ARTICLE

VOLCANICA

Capturing Mayotte's deep magmatic plumbing system and its spatiotemporal evolution with volcano-tectonic seismicity

Aude Lavayssière*[α, β] and Lise Retailleau[α, γ]

[α] Université Paris Cité, Institut de Physique du Globe de Paris, CNRS, 1 rue Jussieu, F-75005 Paris, France.
[β] Geo-Ocean, Univ Brest, CNRS, Ifremer, UMR6538, F-29280 Plouzane, France.
[γ] Observatoire volcanologique du Piton de la Fournaise, Institut de Physique du Globe de Paris, 14 RN3 - Km 27, F-97418 La Plaine des Cafres, La Réunion, France.

Abstract

Since 2018, an unexpected number of earthquakes have been occurring offshore Mayotte, in the Mozambique Channel. They are linked to the eruption of the Fani Maoré submarine volcano. Using a recently developed comprehensive automatic catalog, we explore two years of the volcano-tectonic (VT) seismicity between March 2019 and March 2021, and analyse in detail the active structures of the magmatic plumbing system using ~33,000 events. The VT earthquakes highlight three magma storage zones and two aseismic conduits that have never been observed before. The temporal evolution of the seismicity reveals a probable regime change in March 2020. While before, the plumbing system reacted to the drainage of magma from a deep reservoir and to the migration of magma towards the seafloor, it is now responding to new migrations of fluids and to the redistribution of the stress-load across the system's pre-existing faults. This analysis is key to better understanding long-term volcanism worldwide.

Keywords: Volcano-tectonic seismicity; Mayotte; Submarine volcano; Deep magmatic plumbing system; Temporal evolution.

Submitted: 2023-04-14 | Accepted: 2023-06-27 | Published: 2023-09-13

Editor: O. Lamb | Typesetter: E. Maters

1 Introduction

Changes in seismicity before, during, and after a volcanic eruption indicate changes in the local stress regime, potential fluid migrations, vent openings, or material failure in the plumbing system of a volcano [McNutt and Roman 2015]. The time patterns of the seismicity beneath a volcano, as well as its migration in space, give insights into the dynamics of the magmatic plumbing system and have been used for decades to monitor volcanoes and eruptions [Bell and Kilburn 2012; McNutt and Roman 2015; Power et al. 2020; Matoza et al. 2021; Peltier et al. 2021]. Interpreting seismicity patterns can be challenging as there are multiple sources of earthquakes recorded at volcanoes and they are not necessarily directly associated with the eruptive processes, but also with the regional tectonic context or local stress changes. Most studies focus on pre-eruptive seismicity as it is crucial to determining early warning signs of an eruption and its possible location [Lengliné et al. 2008; Bell and Kilburn 2012; Roman and Cashman 2018]. However, seismicity during and after an eruption informs of potential new vent openings and indicates the eruption's effects on the surrounding system. Hence, it is important to analyse the long-term volcano seismicity in order to monitor and understand long-term eruptions.

Mayotte is the easternmost island of the volcanic Comoros archipelago, between Africa and Madagascar (Figure 1). Historically, the archipelago was considered to result from a hot spot, with the oldest activity at Mayotte and the most recent activity from the Karthala volcano on the westernmost island of Grande Comore [Bachèlery et al. 2016]. Recent studies suggest that the archipelago was formed by a mantle upwelling or by a shear zone separating the Somalia and Lwandle tectonic plates [Famin et al. 2020]. The archipelago undergoes moderate seismic activity with scattered events around the islands [Bertil et al. 2021], apart from seismic swarms linked to eruptions of Karthala volcano [Bachèlery et al. 2016] and more recently in Mayotte.

The 2018 eruption east of Mayotte was preceded by geophysical signals. In May, intense and unexpected seismic activity started with over 130 earthquakes of magnitude (M_L) >4 [Cesca et al. 2020; Lemoine et al. 2020]. This activity was strongly felt by Mayotte's population and sparked much concern. Large subsidence (10–19 cm) and eastward displacement (21–25 cm) of the island were detected a month later and were interpreted as a possible magma withdrawal [e.g. Briole 2018; REVOSIMA 2022]. This hypothesis was further supported by the worldwide detection of a very long-period (VLP) earthquake on 11 November 2018, a type of event generally related to fluid movement [Cesca et al. 2020; Laurent et al. 2020]. The May 2019 MAYOBS1 cruise [Feuillet 2019] led to the discovery of a new submarine volcanic edifice, named Fani Maoré, ~50 km southeast of Mayotte, at the southeast end of an ancient volcanic ridge (Figure 1) [Feuillet et al. 2021].

Only one seismic station [YTMZ, RÉSIF 1995] was recording in Mayotte at the beginning of the seismic swarm. Consequently, the first seismic studies used distant networks [stations in Comoros, Madagascar and Africa, Cesca et al. 2020; Lemoine et al. 2020]. With the expansion of the in-land network in Mayotte from early 2019, Saurel et al. [2022] created the first local seismic catalog for the seismic sequence using manual pickings of the events on both the local land stations and the ocean-bottom seismometers (OBS) network. They located the events with a velocity model rapidly developed while onboard the MAYOBS1 campaign [Feuillet 2019; Saurel et al. 2022]. This dataset contains ~5,000 events from February 2019 to May 2020. Later on, Lavayssière et al. [2022] developed a more precise local 1D velocity model for the active

* aude.lavayssiere@gmail.com

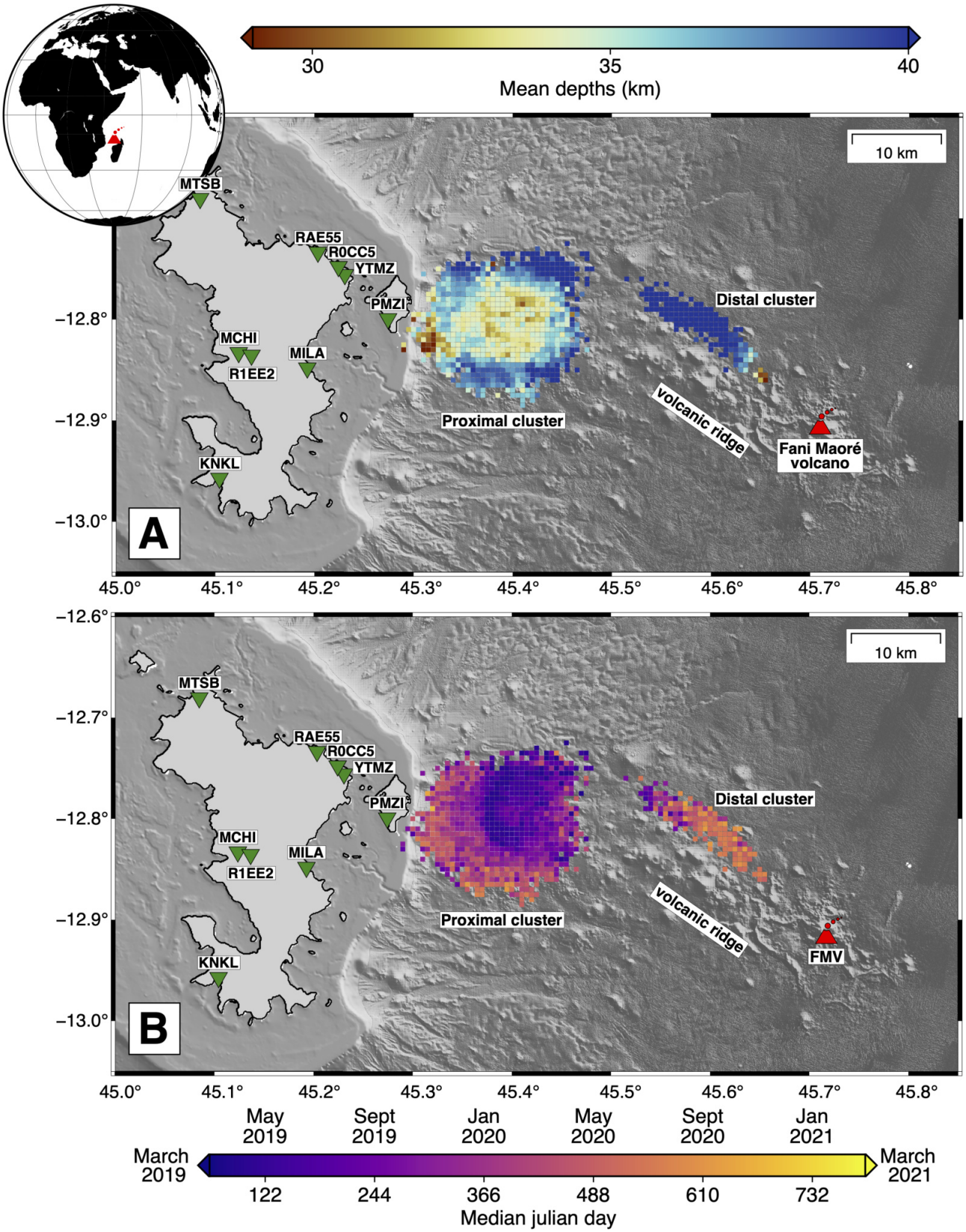

Figure 1: Mayotte's VT seismicity. [A] Average events depths in 1×1×2 km bins. [B] Same as [A] for median Julian days of the events included in the bin. Each node contains at least two events. The land stations used in this study are plotted as inverted green triangles. The inset in [A] shows the study area in a global context (red volcano symbol).

region using the Saurel et al. [2022] catalog, which improved the absolute locations. This velocity model was also built in order to obtain robust locations with only the land-based network. Calculating station corrections to compensate the unidirectional land network geometry, Lavayssière et al. [2022] showed that, with the new model, the locations using the land stations and the locations using land and OBS stations are similar. All these studies [Feuillet 2019; Cesca et al. 2020; Lemoine et al. 2020; Lavayssière et al. 2022; Saurel et al. 2022] showed that the events are distributed in two offshore clusters, a proximal one ~10 km east from Petite Terre island and a distal one ~30 km further east, closer to the Fani Maoré volcano (FMV, Figure 1).

Because it was built manually, the catalog only contains relatively large events (M_c ~2), therefore the smaller events that could reveal details of the active structures were missing. Moreover, the catalog lacks information on the temporal evolution of the seismicity. We note that there is some evidence of temporal behaviour at the very beginning of the crisis, before our analysed period [Cesca et al. 2020; Lemoine et al. 2020; Bertil et al. 2021]. In order to build a more comprehensive catalog, Retailleau et al. [2022] developed an automatic picking of the land-based continuous data, detecting ~8 times more events than previous catalogs. This dataset contains events from March 2019 to March 2021, hence also expanding the previous dataset by almost one year. In contrast with the OBS network, the land-based network has been stable over this time period. This provides more precise results on the seismicity evolution. In their paper, Retailleau et al. [2022] separated volcano-tectonic (VT) and long-period (LP) events through their frequency content. The authors focused on interpreting the LP seismicity in terms of location and time behaviour compared to VT events. They showed that these events are restricted to the central part of the proximal VT seismicity cluster, between 25 and 45 km depth, and occur in swarms [Retailleau et al. 2022].

In the present paper, we complement Retailleau et al. [2022]'s LP analyses by focusing on the VT seismicity of their catalog. We explore its complex temporal and spatial patterns in order to better understand the mechanisms of this uncommonly deep and long-term seismicity. This information is crucial to understand the dynamics of Mayotte's volcanic plumbing system and beyond.

2 A COMPREHENSIVE CATALOG OF AUTOMATICALLY-DETECTED VT SEISMICITY

Mayotte's seismicity consists of different types of events: VT, LP and VLP, a diversity that represents the different source mechanisms. VT earthquakes (2–40 Hz), the most common, are interpreted as mechanical failures while LP (0.5–5 Hz) and VLP (<0.1 Hz) are attributed to resonance of fluid-filled conduits with magma propagation [Chouet 1996; Chouet and Matoza 2013]. For this study, we focus on the VT events from the Retailleau et al. [2022] catalog. This dataset of almost 50,000 VT events was built using the local land network on Mayotte, which recorded from March 2019 to March 2021, and the deep-neural-network-based method PhaseNet [Zhu and Beroza 2019]. The automatic detection allowed the magnitude of completion to be lowered from ~2.5 to ~1. Retailleau et al. [2022] located all detected events with NonLinLoc [Lomax et al. 2000] using the previously-mentioned Lavayssière et al. [2022] local 1D velocity model. Similarly to the previous seismic studies on Mayotte, our catalog shows VT events located in two distinct clusters, both at depths of 25–45 km, but highlights more detailed structures than previous catalogs (Figure 1A).

To avoid bias due to outlier events while acquiring a significant catalog size, we selected well-constrained events with minimum root-mean-square (RMS) and locations errors, yielding a final catalog of 32,827 events* (Figure 2). Due to the land network configuration, the errors in location increase as the events are located further to the east of Mayotte. Thus, we determine different thresholds for the events' selection for the proximal (~5–10 km from the network) and distal (~30–50 km from the network) cluster. For each cluster, we search the location error values with the highest number of events on the error distribution graph. For example, for the longitude errors in the proximal cluster, the error with the highest count of events has 9,073 events (max count line, Figure 2). We calculate 20% of this maximum count—a percentage chosen because it combines a sufficient number of events and consistency in the locations—and we obtain the threshold error value. Following the previous example, we plot the line representing 20% of 9,073 on the distribution graph (20% max count line), and hence identify the longitude error threshold at 6.5 km (Figure 2). We then select all events that have lower errors. Using this process, we determined the following thresholds (Figure 2):

- For the proximal cluster: RMS ≤0.13 s, longitude error ≤6.5 km, latitude error ≤6 km, and depth error ≤6 km;
- For the distal cluster: RMS ≤0.1 s, longitude error ≤10.5 km, latitude error ≤12 km, and depth error ≤19 km.

Figure 3 represents example signals recorded by station MTSB for VT earthquakes in the proximal [A] and distal [B] cluster. Both events have energy in the 1–40 Hz band and clear P- and S-wave arrivals with a few seconds of difference. We show in Figure 4 that the ellipsoids of our locations errors remain relatively large, which is expected considering the azimutal gap of the land network. If we compare with Lavayssière et al. [2022], their catalog shows smaller errors because they used OBS stations that surround the seismicity, resulting in a smaller azimutal gap. Small-size structures (i.e. smaller than the average error estimated at ~4×4×4 km) will be interpreted and discussed in terms of relative locations compared to the rest of the events. We will focus in this study on the significant temporal evolution of the clusters, hence working on their relative locations.

Ultimately, the two clusters are well-defined (Figure 1, Figure 4). The distal cluster is a small linear cluster, aligned in a ~110–130°N direction towards the FMV. The events in this cluster get shallower, up to ~25 km depth, to the southeast, in the direction of the FMV (Figure 1A). These shallowest events are also the most recent of the analysed period (Figure 1B).

*https://figshare.com/s/5bc4338f4e6ed66f7b9a

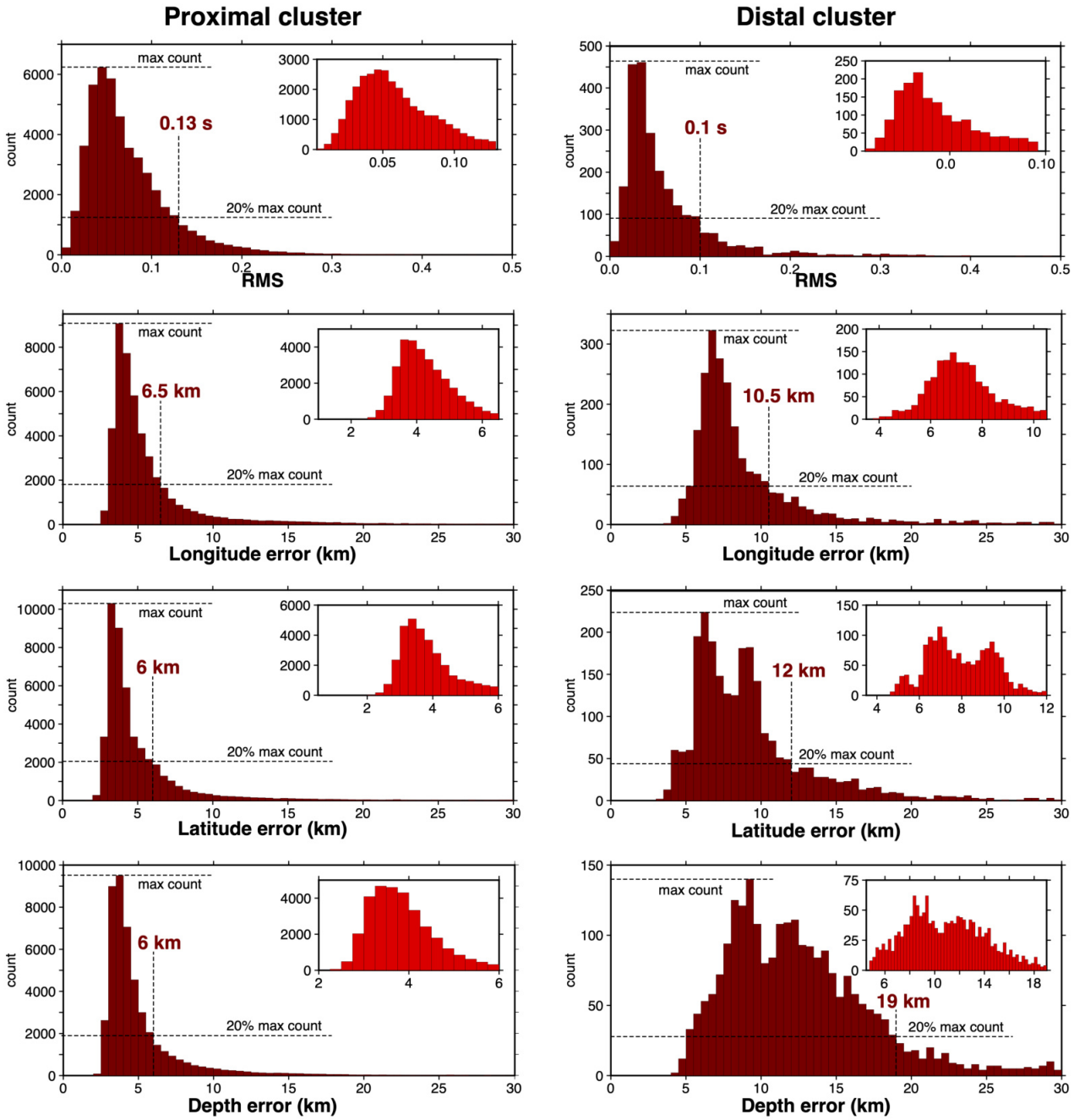

Figure 2: Location errors distribution. Dark red histograms are the errors' distributions before selection of the well-constrained events. The bright red histograms are the errors' distributions after selection. Graphs for the proximal cluster are plotted on the left and on the right for the distal cluster. From top to bottom: RMS, longitude errors, latitude errors and depth errors. See main text for details.

In contrast, the proximal cluster, closest to Petite Terre, represents 95% of the catalog. It has a circular shape horizontally and a complex structure in depth (Figure 1A). Its deepest events are at the edges of the cluster (blue nodes) whereas the shallowest events are located in its center and at the west edge (orange/red nodes). We do not detect any obvious link between depths and temporal evolution for this cluster.

3 Depth of Mayotte's active magmatic plumbing system

Seismicity at volcanoes is generally dominated by shallow events, in the upper crust and below the surface edifices, reflecting the fracturing generated by magma intrusions towards the surface [Ratdomopurbo and Poupinet 2000; Roman et al. 2008]. In contrast, apart from the first few months of activity

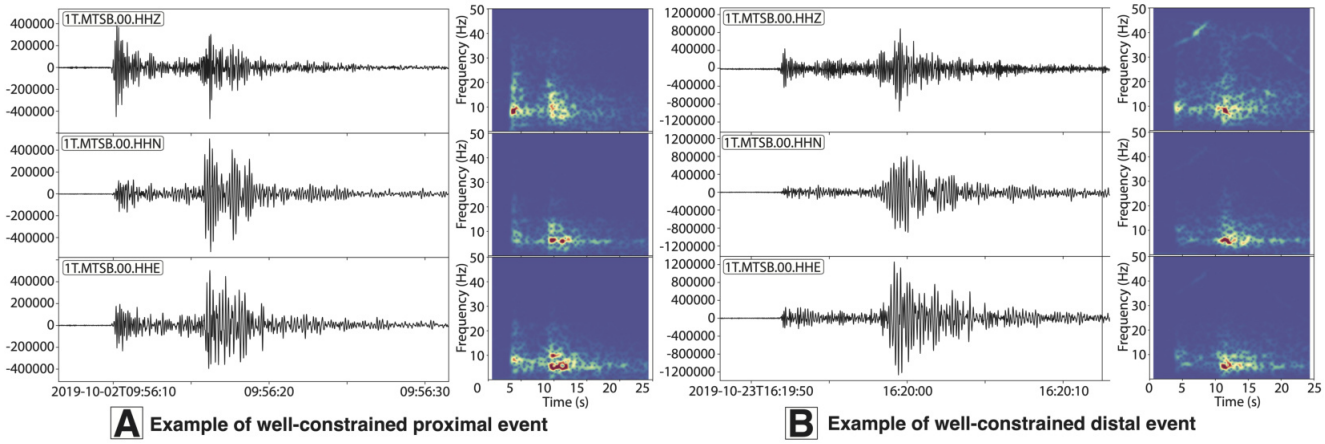

Figure 3: Examples of three-component waveforms and spectrograms of an event from the proximal [A] and the distal [B] cluster.

that led to the start of the eruption [Cesca et al. 2020; Lemoine et al. 2020], Mayotte earthquakes have been confined between 25 and 45 km depth from March 2019 to March 2021. It has remained this deep since then [REVOSIMA 2022]. Saurel et al. [2022] tested different velocity models for their earthquakes locations and found consistency in the resulting depth ranges. Moreover, all studies using different location processes also found similar depths [Cesca et al. 2020; Lemoine et al. 2020; Bertil et al. 2021; Feuillet et al. 2021; Lavayssière et al. 2022]. The Moho in the region surrounding Mayotte has been estimated at 17–27 km depth [Dofal et al. 2021], consistent with the 1D velocity model by Lavayssière et al. [2022]. From these estimations, Mayotte events occur entirely in the upper mantle. These depths are unexpected due to the dominant ductile nature of the upper mantle [McKenzie et al. 2005]. For a ductile material to become brittle at such depths, very high strain rates and/or increased pore pressure are necessary. This is possible in volcanic systems where there are rheological changes (composition and/or temperature) in specific areas, where important movements of melt can occur, increasing the strain rate enough for shear failure to occur, and where gases contained in the melt can exsolve. The long-term character of Mayotte deep seismicity differs from the transient deep VT and LP seismicity detected at other magmatic systems, generally interpreted as evidence of magma replenishment in the deep parts of the magmatic systems [Wright and Klein 2006; Michon et al. 2015; Shapiro et al. 2017; Hotovec-Ellis et al. 2018; D'Auria et al. 2022; Wilding et al. 2022]. The authors of these studies interpret that deep earthquakes can be linked to lithospheric dynamics (i.e. plate movements, melt migrations, plume, etc.), to adjustments of the lithosphere from the load of the surface edifices, to flank movements, or to fluid migrations in conduits and reservoirs, all processes also interacting with regional stresses.

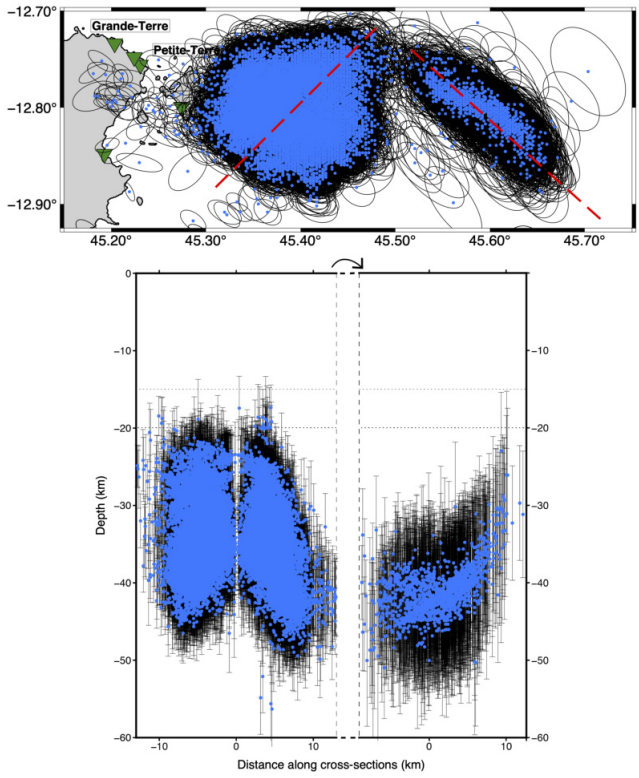

Figure 4: [Top] Map of the two seismicity clusters after selection with the maximum likelihood locations in blue and associated horizontal ellipsoidal errors as black ellipses. Red dashed lines are the traces of the cross-section below. [Bottom] Cross-section across both clusters with the maximum likelihood locations in blue and associated depth errors as black lines.

The earthquakes are confined at slightly different depths for the two clusters. The proximal cluster seismicity starts at ~22 km depth, and this limit slowly becomes deeper from May 2020 (Figure 5C). On the other hand, the distal cluster events were blocked at ~38 km before mid-March 2020, with only a few events reaching shallower depths, and at ~30 km after mid-March 2020 (Figure 5C). The absence of shallow seismicity could partly be due to the sole use of the land network, thus limiting small event detection. Indeed, while we detect events of M_L ≤0.5 in the proximal cluster, we do not detect events of M_L <1 around the distal cluster (Figure 5B). However, shallow events were not detected either on previous studies using OBS data [Saurel et al. 2022]. Shallow events have been identified at the beginning of the swarm, before our study period, with only few and regional stations avail-

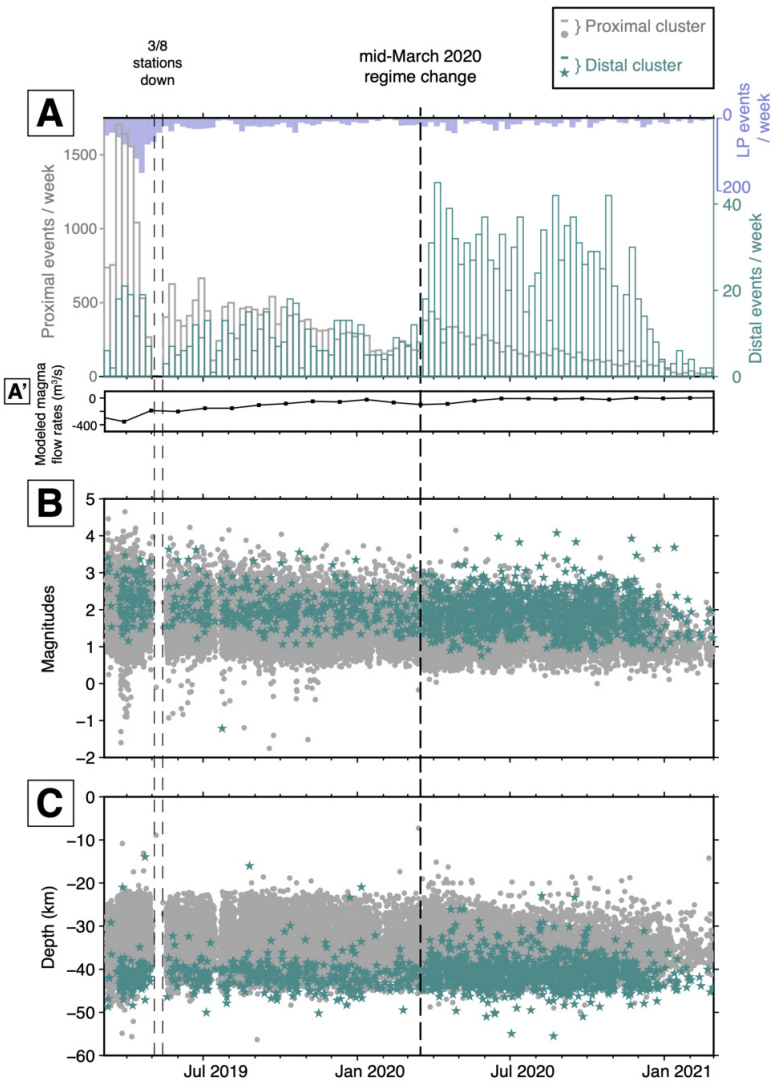

Figure 5: Mayotte's VT seismicity over time for the proximal (gray) and distal (cyan) clusters. [A] Evolution of the number of events in the proximal and distal clusters per week. Evolution of the LP events is indicated in blue. Evolution of modelled flow rates from GNSS data is indicated in A' [Beauducel et al. 2020; Peltier et al. 2021]. [B] Evolution of the events' magnitudes. [C] Evolution of the events' depth.

able at the time. Such shallow events have not been observed since the network was improved. During this period the activity was strongest and magma propagated towards the surface [Cesca et al. 2020; Lemoine et al. 2020], with the largest estimated flux rates in late 2018 [Mittal et al. 2022; Peltier et al. 2022]. Consequently, the medium could have been sufficiently reopened during this first stage and magma could have propagated aseismically later on. We note that these early shallow events were located with a scattered and distant land network and lack precision in depth. Consequently, they may not be shallower than events in our catalog. If this is the case, then magma has been propagating aseismicially in the crust since the beginning of the eruption. Petrological analyses from dredged magma samples have suggested the presence of magma lenses at ~17 ± 6 km depth and the stalling of magma above 20 km depth, depths at which basanitic magma evolves to phonolite [Berthod et al. 2021a]. The lack of shallow seismicity in the proximal region could hence be explained by an upper crust too fractured and ductile for shear failure to occur, as is also suggested by tomography [Foix et al. 2021] and by the numerous cones on the seafloor, signs that previous eruptions have significantly fractured the crust.

4 Mayotte's complex magma plumbing system

During volcanic eruptions, the crust and lithosphere experience a physical transformation and seismicity occurs when the build-up stress of the plumbing system and surrounding region is suddenly released, either because of propagation of hydrothermal and/or magmatic fluids or because of deformation of the reservoir. Thus, it is common to interpret VT earthquakes as the reaction of the solid Earth to the migrations of magmatic fluids towards the volcanic vents and changes in the stress field. However, the absence of VT seismicity in a region surrounded by seismic activity is also used as an in-

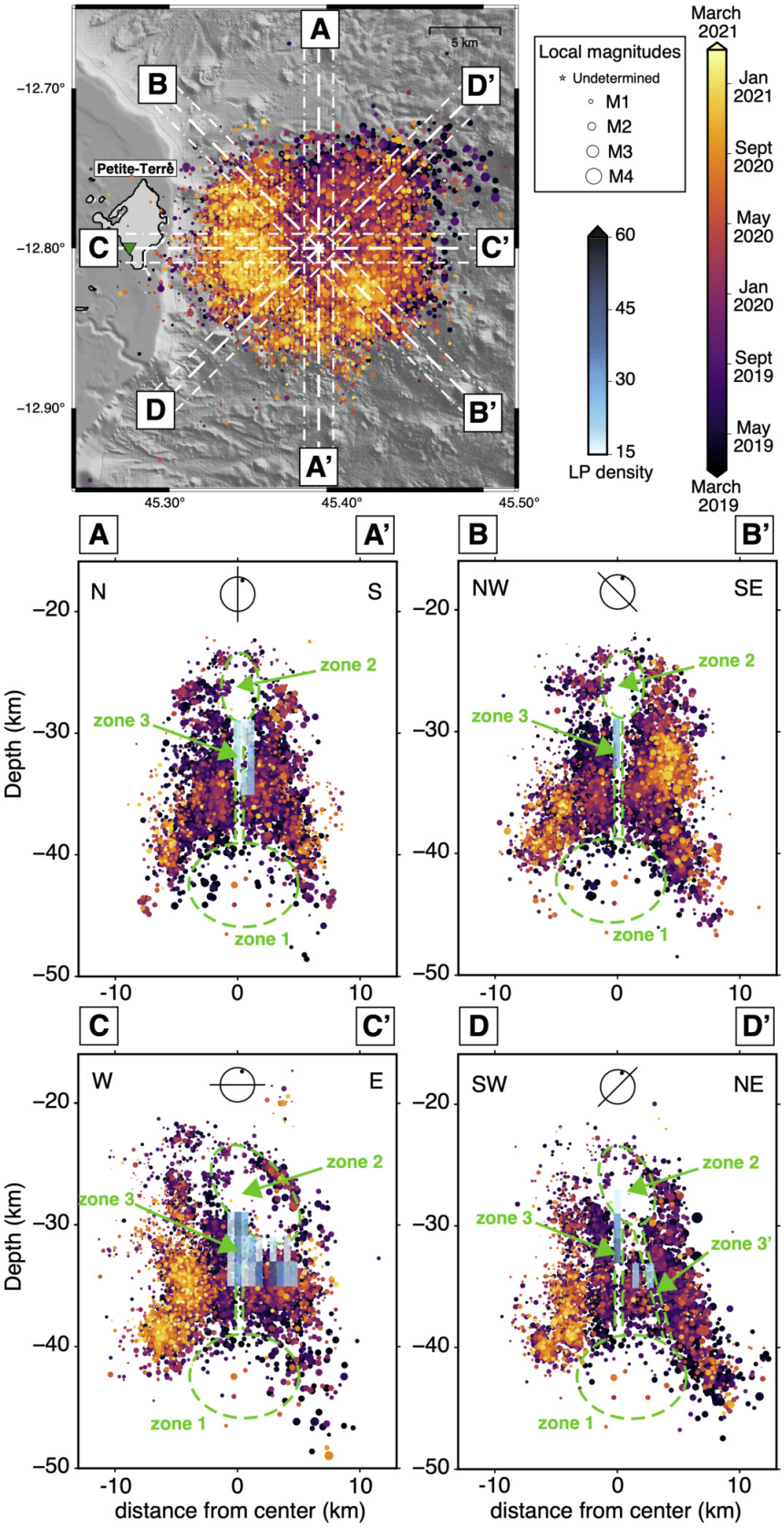

Figure 6: Spatio-temporal evolution of the proximal cluster. Earthquakes are colour-coded by time and sized by magnitudes. Traces of the cross-sections are lettered and indicated on the map. Density of LP events in bins of 0.5×0.5×2 km is also indicated on each cross-section, with only bins containing at least 15 events plotted. Zones of interest are indicated (green dashed lines) and discussed in the main text.

dication of a region of potential magma storage [Jiménez et al. 1999; Hotovec-Ellis et al. 2018; Illsley-Kemp et al. 2021]. These gaps inside a seismically-active zone appear because reservoirs are too hot and ductile for shear failure to occur. On the other hand, the host rocks at the limit of the reservoir break because of escaping fluids or because deformation of the walls induces failure. These gaps can be truly aseismic or they could be a zone of low-magnitude seismicity (i.e. below detection limit) or a zone of unaccounted-for velocity change that biases locations away from this region. In this section we analyse the spatial distribution of the seismicity to infer such structures in the Mayotte volcanic system.

The complex shape of the proximal cluster provides evidence for several seismicity gaps inside active structures. The bottom part of the cluster is shallower at the center (~40 km depth) and deeper on the sides (~45 km depth), with some scattered events in the middle (zone 1, Figure 6). Geobarometry results on recently emitted lavas at the FMV estimated the magma's origin at depths >40 km [Berthod et al. 2021b] and other studies proposed the presence of a magma reservoir below the proximal cluster [Feuillet et al. 2021; Lavayssière et al. 2022]. Consequently, the distribution of the bottom proximal seismicity seems to delimit the extent of a potential reservoir to a size of ~10×10×5 km. Deformation studies also modelled the main deflating reservoir at this same depth of 45 km, although the horizontal location does not match [Mittal et al. 2022; Peltier et al. 2022]. The drainage/replenishment of this deep reservoir could have induced the fracturing of pre-existing faults around it.

Our catalog show newly observed and clear structures inside the proximal cluster. Two types of aseismic zones, spherical and linear, surrounded by seismicity, persist between March 2019 and March 2021 (zones 2 and 3, Figure 6). One of those is a spheroidal gap located at the top of the cluster at ~25–30 km depth (zone 2, Figure 6). This feature is similar in size (~2×5×5 km) to our average error in location but nevertheless reveals a clear gap in relative locations. This zone is evocative of a magma storage zone and our catalog shows the 3D geometry of this potential reservoir in detail. Our new observations also show that in relative locations this gap seems to have expanded with time (Figure 6). This migration of the seismicity around a potential reservoir could fit with the presence of a porous magma mush adjacent to a visco-elastic reservoir, which was suggested by a new conceptual model [Mittal et al. 2022]. Similar to the deep reservoir, the deformation of this central mush zone could have built up pressure around its sides and triggered the (re)opening of small faults.

The other type of aseismic zone highlighted by the proximal seismicity is a linear structure at the center of the cluster that had not been observed in previous Fani Maoré seismicity studies (zone 3, Figure 6). Note that this feature is clear but small (less than ~1 km across for ~10 km long) compared to our location errors. It starts at the bottom of the spheroidal gap and extends to the bottom of the cluster. On the SW-NE cross-section, a second linear gap is visible, dipping towards the northeast (zone 3', cross-section D, Figure 6). LP events are located almost exclusively in those linear VT gaps (Figure 6). The same location procedure was used to locate both types of events. Consequently, if there are biases due to the geomety of the stations, they are the same for VT and LP earthquakes [Retailleau et al. 2022]. Thus, even if our absolute locations may be slightly incorrect, we can interpret the LP locations relative to the VT locations. The occurrence of LP earthquakes inside gaps of VT seismicity was previously interpreted as the presence of magmatic fluids, as LP events are indicative of a propagation through a fluid-rich medium [Hotovec-Ellis et al. 2018; Retailleau et al. 2022]. If the linear structures highlighted here represent conduits, both the presence of LP and the absence of VT seismicity could be explained by the intrusion of fluids in a pre-exisitng already-fractured conduit system.

The proximal cluster started being active after the distal cluster, which is related to the dike propagation [Feuillet 2019; Cesca et al. 2020; Lemoine et al. 2020]. Consequently, we expect the two clusters to be linked. However there is no seismicity at any depth in between the clusters (Figure 1). This can be explained if the magmatic conduits have already been sufficiently fractured and the magma propagation does not fracture the medium anymore. It is possible that seismicity occurred previously in this region but has not been properly located due to the lack of a local seismic network. However, the distal cluster provides evidence for fracturing further along the propagation path. Another possibility for the absence of seismicity in between the clusters is the presence of another active magmatic reservoir, as this aseismic region is closer in horizontal location to the main reservoir modelled by deformation studies [Mittal et al. 2022; Peltier et al. 2022] (Figure 7).

These four aseismic regions suggest a complex active system with several storage zones and connections where magmatic fluids might migrate/have migrated in the past (Figure 7). These migrations could have reactivated a pre-existing fault system by disturbing the local stress-field [Jiménez et al. 1999; Michon et al. 2015; Hudson et al. 2017; Burgess and Roman 2021; Ortega-Romo and Chen 2021]. The combination of several potential reservoirs and this fault system would explain the complex seismicity of the proximal cluster. Melt can move at significant pressure, sufficient to induce brittle failure of the host rock, and the fluid intruding into the resulting cracks can provide a volumetric increase for the melt to continue moving [Michon et al. 2015; Hudson et al. 2017]. This correlates with our observations for the distal cluster as well as observations of transient deep seismicity beneath volcanoes [Michon et al. 2015]. There are also several observations of VT earthquakes triggered by an increase in volatiles, mainly CO_2, exsolved from the melt by decompression as melt rises through depths [Hudson et al. 2017; Hotovec-Ellis et al. 2018] or by crystallisation of melt in situ [Tait et al. 1989; Ratdomopurbo and Poupinet 2000], and creating an overpressure on the system [Hudson et al. 2017]. That might explain the distribution of the seismicity around melt conduits and storage zones, such as the proximal system in Mayotte and, more generally, the seismicity beneath erupting volcanoes. We note that these movements of fluids in the system could be linked to the observations of discrete degassing at the seafloor above the proximal cluster [MAYOBS campaigns, Rinnert et al. 2019; REVOSIMA 2022], and to LP and VLP events that have been detected and located at or above the proximal cluster [Laurent

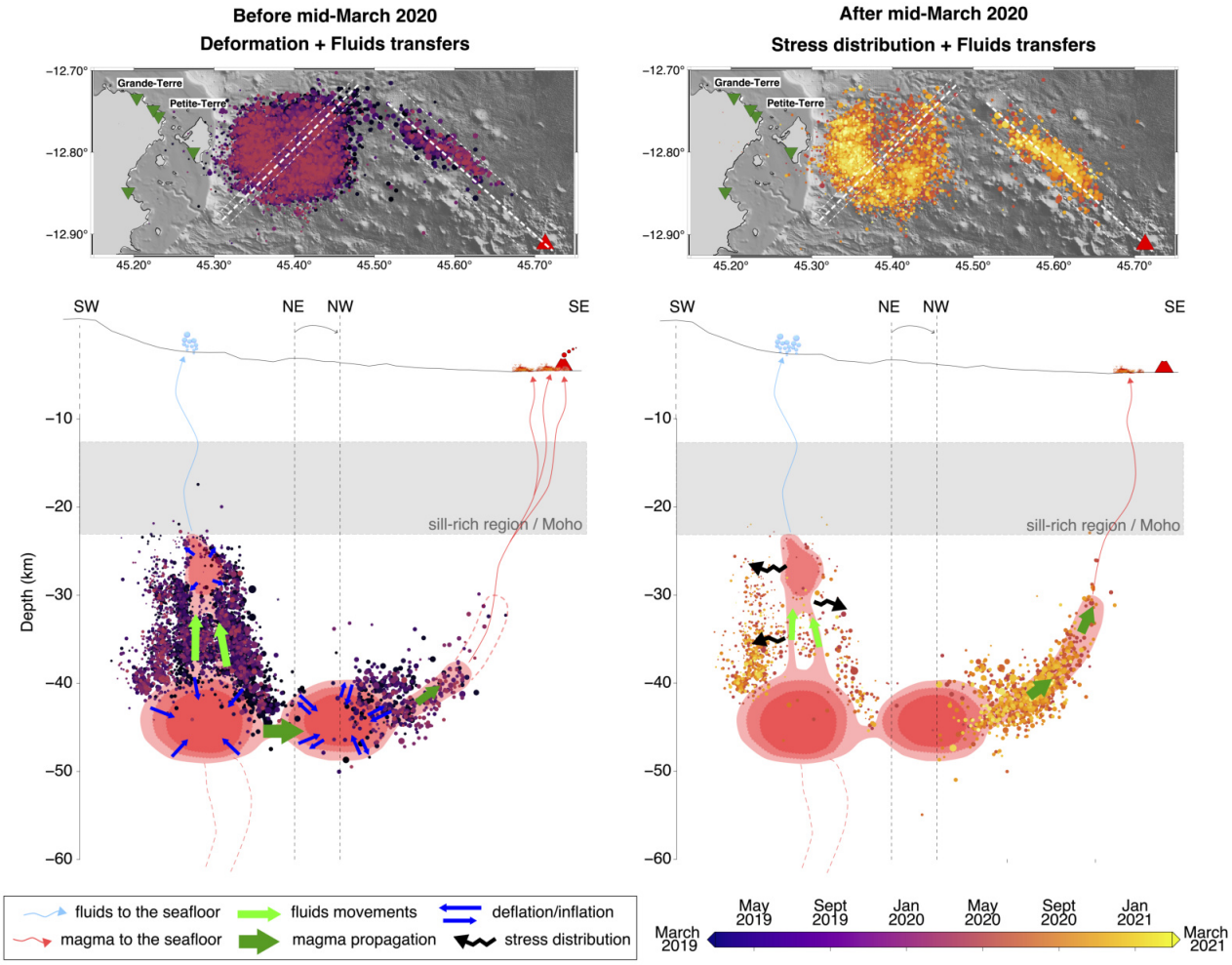

Figure 7: Schematic interpretation of the mid-March 2020 regime change. Cross-section across both clusters with events colour-coded by time and sized by magnitudes before (left) and after (right) mid-March 2020. Traces of the cross-sections are indicated on the respective maps. Zones of interest are discussed in the main text. A region (grey layer) combining estimated Moho depths [Dofal et al. 2021; Lavayssière et al. 2022] and presence of magmatic sills [Berthod et al. 2021a], as well as the locations of observed fluid escapes at the seafloor [REVOSIMA 2022], are also indicated.

et al. 2020; Retailleau et al. 2022]. When melt or gases rise through an already-existing faulting system, the favorably oriented faults can be reactivated by the same processes that creates new faults, and with a lower stress-load needed [Michon et al. 2015; Hudson et al. 2017; Burgess and Roman 2021]. As our study area contains an underwater volcanic ridge [Feuillet et al. 2021], a pre-existing plumbing system is highly likely. Hence, the seismogenic structures observed during Mayotte eruption are probably reflecting the part of the pre-existing fault system subjected to increased pressure, but not the full extent of the magmatic plumbing system.

5 Evolution of the seismicity and evidence for a regime change in 2020

Overall, Mayotte's seismicity has been decreasing since 2019 (Figure 5A) [REVOSIMA 2022]. In detail, during the period we analyse, the temporal evolution differs between the two clusters, though there is also evidence of simultaneous changes in activity. Note that in the following section, the distribution of the events is discussed in terms of relative location rather than absolute.

From studies on the early part of the activity [Cesca et al. 2020; Lemoine et al. 2020; Bertil et al. 2021], we know that the distal cluster was the first to appear in May 2018 and has been linked to magma migration towards the FMV. Its seismicity has been interpreted as the (re)activation of faults by the propagation of a dyke [Cesca et al. 2020; Morales-Yáñez et al. 2022]. From our observations, between March 2019 and early 2020, the activity in this cluster was relatively constant with ~10 events per week on average (Figure 5A). However, there was a significant change between mid-March 2020 and January 2021 with an increase in activity that coincides with several events of M_L 3–4, some felt in Mayotte [REVOSIMA 2022] (Figure 5B). It also coincides with the occurrence of slightly shallower events relative to the others (Figure 5C). The dominant activity in the distal cluster from mid-March 2020 to early 2021 is distributed in a banana shape that shal-

lows to the southeast, in a direction towards the northwest of the FMV (Figure 7). This distribution suggests a new migration of magma and/or fluids, consistent with a change in modelled magma flow rates between January and June 2020 (Figure 5A') [Mittal et al. 2022]. This new migration either stopped at Moho depths or reached the surface aseismically (i.e. Section 3). Punctual evolution of the active lava flows was observed with the MAYOBS oceanographic campaigns [Rinnert et al. 2019]. Besides the FMV, active lava flows have been observed to the south of the edifice (May-June 2019) and to the west (June-July 2019). Between July 2019 and January 2021, the active lava flows have been focused to the northwest of the FMV and between early 2020 and early 2021 an increase of the height of these northwest lava flows have been detected [Rinnert et al. 2019; REVOSIMA 2022]. These observations would support aseismic migrations reaching the seafloor to the northwest of the FMV after mid-March 2020 (Figure 7).

The proximal cluster started being active after a few months of the eruption and followed GNSS observations indicating a deflation in the region. This suggests the drainage of a main reservoir at depth [Cesca et al. 2020; Lemoine et al. 2020; Feuillet et al. 2021; Mittal et al. 2022]. Some authors interpret the 30–50 km-depth proximal seismicity as dominant major faults above a draining reservoir, similar to ring faults [Lavayssière et al. 2022], and a caldera collapse/piston system [Feuillet et al. 2021], or as critically-stressed faults that reacted to poroelastic stress changes in a magmatic mush zone [Mittal et al. 2022]. Such a deep seismic cluster above a lithospheric reservoir has also been observed at La Palma during the 2021 Tajogaite eruption, although it was accompanied by shallower seismicity and the mantle seismicity was transient [D'Auria et al. 2022]. D'Auria et al. [2022] suggested similar explanations for the complexity of the earthquakes distribution: magma compression with increased pressure due to magma being pushed downward by a collapse of the crustal material and upward by magma ascending from the mantle; or stress propagation due to magma withdrawal. However, the Tajogaite eruption was associated with visible morphological observations of the caldera collapse, a mechanism well known when calderas are associated with shallow reservoirs in the crust. This collapse mechanism is highly debated in relation to Mayotte. First, there are no morphological observations at the surface. Moreover, the observed seismicity and interpreted main reservoir are much deeper compared to suggested collapse cases. With the smaller magnitude of completeness reached with our catalog, we show a more complex and wider system. In Hawai'i, a deep magmatic plumbing system has been evidenced with the same deep-learning earthquakes detection method we used here [Wilding et al. 2022]. They showed a deep VT cluster associated with LP swarms approximately 30 km from the Kīlauea summit and caldera. However, this mantle seismicity was transient in their case. They interpreted the VT and LP events as resulting from magma infiltrations in a deep sill complex, connected to the shallower plumbing system of the Hawaiian volcanoes. The similarities in the distance from the eruption as well as the presence of LP events inside a VT cluster between Hawai'i and Mayotte hints that these are more common structures and mechanisms than previously thought. It shows the importance of better detection and location methods, and the difficulty in interpreting large complex catalogs.

The proximal activity decreased significantly in April-May 2019 and most of it continued to decrease more slowly since then with ~25 events per week in March 2021 (Figure 5A). However, the early-2020 change in activity we detected in the distal cluster is also visible in the proximal cluster with a slight increase in the number of events, some shallower events (<20 km), a few larger earthquakes (M_L >3) and several felt earthquakes [REVOSIMA 2022] (Figure 5). This suggests that the proximal and distal clusters are linked.

While the number of VT events varies only slightly and their overall magnitudes do not change in the proximal cluster in March 2020, there is a significant change in the active structures below ~30 km depth (Figure 7). Several groups of VT events highlighted by our catalog have interesting evolution patterns. A well-defined near-vertical linear group of seismicity stands out in the proximal cluster, in the center west (cross section D, Figure 6, Figure 7A). This structure is fully inactive by March 2020 (Figure 7B). It is located at the west side of the vertical central aseismic conduit mentioned previously (zone 3, Figure 6, Section 4). The east side of the second aseismic conduit (zone 3', Figure 6) is also accompanied by aligned seismicity, though this group is less defined and more distributed spatially. The seismicity that coincides with the sides of the second conduit disappears after March 2020 but the rest of this group is still active, particularly in the southwest (Figure 7B). In between the two aseismic conduits, there is seismic activity as well, still active after March 2020 but in lesser numbers. These seismicity groups at the sides of the aseismic conduits may be explained by the reactivation of faults due to the propagation of magmatic fluids that increased pore fluid pressure. Their disapearance coincides with the end of detectable deformation [Mittal et al. 2022; Peltier et al. 2022; REVOSIMA 2022] and hence also hints at mechanisms related to the stress imposed by the deformation of the complex reservoir system. We detect a small swarm of LP occurring in early 2020 (Figure 5A). The LP seismicity slowly decreases after November 2019 until this peak that coincides with the slight increase in proximal VT, suggesting new but small fluids migrations in the proximal magmatic conduits. The disappearance of these groups of seismicity after mid-March 2020 makes them representative of the main processes occurring in the proximal cluster in the first part of the eruption. Finally, the rest of the proximal seismicity (Figure 7B), which stayed active after March 2020, is more scattered. The central part of the proximal seismicity has been slowly disappearing and the more recent earthquakes are mainly at the sides (Figure 7). This might indicate that the stress load is being slowly redistributed around the pre-existing volcanic plumbing system. We do not see any specific change in March 2020 for this part of the proximal seismicity. We note two main regions that are still intensely active after mid-March 2020: the west part, closer in horizontal distance to Mayotte, between 30 and 45 km depth (cross section C, Figure 6), and the southeast part, between 30 and 35 km (cross section B, Figure 6).

The mid-March 2020 change in activity hints at a regime change for the system. If previously the system mainly reacted to the drainage of the deep reservoir, it is now reacting to the redistribution of the stress and to new migration of fluids at depths, without any new detectable deformation [REVOSIMA 2022]. Such surges of activity during eruptions have been seen at other volcanoes [Jiménez et al. 1999; Burgess and Roman 2021] and are important to understand for better monitoring and forecasting of long-term eruptions. Several surges of seismicity were detected between 2015 and 2020 in Hawai'i [Burgess and Roman 2021] and their differences were explained by a change in the nature of the intruded rock: intrusion into a ductile and well-developed system associated with minimal seismicity and intrusion in a non-developed system (or intrusion too large to be accommodated by the already-existing conduit system). In 2019 in particular, ~one year after the end of a large caldera collapse event at Kīlauea, a mantle-deep earthquake swarm was observed ~30 km away from the caldera [Wilding et al. 2022]. This last surge seems interestingly analogous to the Mayotte seismic sequence with deep VT earthquakes and complex lateral movements, but differs by its transient nature. Surges can also occur during one eruption [Jiménez et al. 1999]. Cyclic episodes of earthquake swarms during the 1982 El Chichón eruption were related to progressive filling of the volcanic conduits due to renewed pressure. Finally, surges of LP activity, such as the swarm we observed in the proximal cluster early 2020, were also observed beneath volcanoes and are generally related to new magmatic unrest. Hence, the regime change we observed in mid-March 2020 is probably a combination of changes: end of the draining of the deep reservoir but new migrations of fluids in the volcanic system's conduits, and it hints at an interconnectivity inside the plumbing system that has rarely been observed before.

6 Conclusions

We explore Mayotte's deep magmatic system using a two-year comprehensive catalog of VT seismicity. This catalog was obtained with automatic detection procedures and re-locations of the events between March 2019 and March 2021. The evolution of this VT seismicity through time provides insights into the dynamics of the magmatic plumbing system.

We showed that the VT seismicity is complex in Mayotte, with different processes at play that modified the local state of stress. We propose three potential magma storage zones, some connected by aseismic conduits, and interpret that the migration of magmatic fluids overpressured the system and triggered the reactivation of pre-existing faults. These fluids either rise aseismically from ~30 km depth due to an already-fractured crust and/or are stalling at different depths due to the presence of pre-existing magma accumulations zones as well as specific tectonic layers such as the Moho.

We also show that magma release from a deep reservoir is the main process triggering the VT seismicity until mid-March 2020 with the reactivation of the pre-existing fault system. After mid-March 2020 however, the system reacts to new magmatic fluids migrations at depth and to the redistribution of the stress load across the pre-existing fault system.

Mayotte's seismicity has generally decreased since 2019 and at the end of our time period, in March 2021, events are very deep but only ~5 km from Petite Terre island in horizontal distance, still posing a risk for Mayotte's population. It is essential to keep monitoring the seismicity in this region.

Author Contributions

A. Lavayssière and L. Retailleau worked together on the manuscript and on the interpretation of the results. A. Lavayssière processed the data and created the figures.

Acknowledgements

Since June 2019, Mayotte eruption monitoring is funded by le Ministère de l'Enseignement Supérieur, de la Recherche et de l'Innovation (MESRI), le Ministère de la Transition Ecologique (MTE) and le Ministère des Outremers (MOM) with the support of le Ministère de l'Intérieur (MI) and le Ministère des Armées (MINARM) through the REVOSIMA (Réseau de surveillance volcanologique et sismologique de Mayotte; Mayotte Volcanological And Seismological Monitoring Network). AL was partly funded by the European Union's Horizon 2020 research and innovation program under Eurovolc projet (grant agreement No 731070). GMT [Wessel et al. 2019] and `ObsPy` [Beyreuther et al. 2010] were used to create the figures. The authors thank the reviewers and the editor for their reviews which helped improve the manuscript.

Data Availability

The dataset of well-constrained earthquakes used in this paper is available here: https://figshare.com/s/5bc4338f4e6ed66f7b9a.

Copyright notice

References

Bachèlery, P., J. Morin, N. Villeneuve, H. Soulé, H. Nassor, and A. R. Ali (2016). "Structure and Eruptive History of Karthala Volcano". *Active Volcanoes of the World*. Edited by P. Bachelery, J.-F. Lenat, A. Di Muro, and L. Michon. Berlin, Heidelberg: Springer Berlin Heidelberg. Chapter Active Vol, pages 345–366. ISBN: 978-3-642-31395-0. DOI: 10.1007/978-3-642-31395-0{_}22.

Beauducel, F., D. Lafon, X. Béguin, J. M. Saurel, A. Bosson, D. Mallarino, P. Boissier, C. Brunet, A. Lemarchand, C. Anténor-Habazac, A. Nercessian, and A. A. Fahmi (2020). "WebObs: The Volcano Observatories Missing Link Between Research and Real-Time Monitoring". *Frontiers in Earth Science* 8(February), pages 1–22. DOI: 10.3389/feart.2020.00048.

Bell, A. F. and C. R. J. Kilburn (2012). "Precursors to dyke-fed eruptions at basaltic volcanoes: insights from patterns of volcano-tectonic seismicity at Kilauea volcano, Hawaii". *Bulletin of Volcanology* 74(2), pages 325–339. DOI: 10.1007/s00445-011-0519-3.

Berthod, C., E. Médard, P. Bachèlery, L. Gurioli, A. Di Muro, A. Peltier, J.-C. Komorowski, M. Benbakkar, J.-L. Devidal, and J. Langlade (2021a). "The 2018-ongoing Mayotte submarine eruption: Magma migration imaged by petrological monitoring". *Earth and Planetary Science Letters* 571, page 117085. DOI: 10.1016/j.epsl.2021.117085.

Berthod, C., E. Médard, A. Di Muro, T. Hassen Ali, L. Gurioli, C. Chauvel, J.-C. Komorowski, P. Bachèlery, A. Peltier, and M. Benbakkar (2021b). "Mantle xenolith-bearing phonolites and basanites feed the active volcanic ridge of Mayotte (Comoros archipelago, SW Indian Ocean)". *Contributions to Mineralogy and Petrology* 176(10), pages 1–24.

Bertil, D., N. Mercury, C. Doubre, A. Lemoine, and J. Van der Woerd (2021). "The unexpected Mayotte 2018–2020 seismic sequence: a reappraisal of the regional seismicity of the Comoros". *Comptes Rendus. Géoscience* 353(S1). DOI: 10.5802/crgeos.79.

Beyreuther, M., R. Barsch, L. Krischer, T. Megies, Y. Behr, and J. Wassermann (2010). "ObsPy: A Python toolbox for seismology". *Seismological Research Letters* 81(3), pages 530–533. DOI: 10.1785/gssrl.81.3.530.

Briole, P. (2018). *Note sur la crise tellurique en cours à Mayotte*. http://volcano.iterre.fr/wp-content/uploads/2018/11/mayotte_note_deformation_GPS_20181112a.pdf 20181112a. ENS Geosciences – Volcanology, Paris.

Burgess, M. K. and D. C. Roman (2021). "Ongoing (2015-) Magma Surge in the Upper Mantle Beneath the Island of Hawaii". *Geophysical Research Letters* 48(7), e2020GL091096. DOI: 10.1029/2020GL091096.

Cesca, S., J. Letort, H. N. T. Razafindrakoto, S. Heimann, E. Rivalta, M. P. Isken, M. Nikkhoo, L. Passarelli, G. M. Petersen, and F. Cotton (2020). "Drainage of a deep magma reservoir near Mayotte inferred from seismicity and deformation". *Nature Geoscience* 13(1), pages 87–93. DOI: 10.1038/s41561-019-0505-5.

Chouet, B. A. (1996). "Long-period volcano seismicity: its source and use in eruption forecasting". *Nature* 380(6572), pages 309–316. DOI: 10.1038/380309a0.

Chouet, B. A. and R. S. Matoza (2013). "A multi-decadal view of seismic methods for detecting precursors of magma movement and eruption". *Journal of Volcanology and Geothermal Research* 252, pages 108–175. DOI: 10.1016/j.jvolgeores.2012.11.013.

D'Auria, L., I. Koulakov, J. Prudencio, I. Cabrera-Pérez, J. M. Ibáñez, J. Barrancos, R. García-Hernández, D. Martínez van Dorth, G. D. Padilla, M. Przeor, V. Ortega, P. Hernández, and N. M. Peréz (2022). "Rapid magma ascent beneath La Palma revealed by seismic tomography". *Scientific Reports* 12(1), pages 1–13. DOI: 10.1038/s41598-022-21818-9.

Dofal, A., F. R. Fontaine, L. Michon, G. Barruol, and H. Tkalčić (2021). "Nature of the crust beneath the islands of the Mozambique Channel: Constraints from receiver functions". *Journal of African Earth Sciences* 184, page 104379. DOI: 10.1016/j.jafrearsci.2021.104379.

Famin, V., L. Michon, and A. Bourhane (2020). "The Comoros archipelago: a right-lateral transform boundary between the Somalia and Lwandle plates". *Tectonophysics* 789, page 228539. DOI: 10.1016/j.tecto.2020.228539.

Feuillet, N. (2019). *MAYOBS1 cruise, RV Marion Dufresne*. DOI: 10.17600/18001217.

Feuillet, N., S. Jorry, W. C. Crawford, C. Deplus, I. Thinon, E. Jacques, J. M. Saurel, A. Lemoine, F. Paquet, and C. Satriano (2021). "Birth of a large volcanic edifice offshore Mayotte via lithosphere-scale dyke intrusion". *Nature Geoscience* 14(10), pages 787–795. DOI: 10.1038/s41561-021-00809-x.

Foix, O., C. Aiken, J.-M. Saurel, N. Feuillet, S. J. Jorry, E. Rinnert, and I. Thinon (2021). "Offshore Mayotte volcanic plumbing revealed by local passive tomography". *Journal of Volcanology and Geothermal Research* 420, page 107395. DOI: 10.1016/j.jvolgeores.2021.107395.

Hotovec-Ellis, A. J., D. R. Shelly, D. P. Hill, A. M. Pitt, P. B. Dawson, and B. A. Chouet (2018). "Deep fluid pathways beneath mammoth mountain, California, illuminated by migrating earthquake swarms". *Science Advances* 4(8). DOI: 10.1126/sciadv.aat5258.

Hudson, T. S., R. S. White, T. Greenfield, T. Ágústsdóttir, A. Brisbourne, and R. G. Green (2017). "Deep crustal melt plumbing of Bárðarbunga volcano, Iceland". *Geophysical Research Letters* 44(17), pages 8785–8794. DOI: 10.1002/2017GL074749.

Illsley-Kemp, F., S. J. Barker, C. J. Wilson, C. J. Chamberlain, S. Hreinsdóttir, S. Ellis, I. J. Hamling, M. K. Savage, E. R. Mestel, and F. B. Wadsworth (2021). "Volcanic Unrest at Taupō Volcano in 2019: Causes, Mechanisms and Implications". *Geochemistry, Geophysics, Geosystems* 22(6), pages 1–27. DOI: 10.1029/2021GC009803.

Jiménez, Z., V. H. Espíndola, and J. M. Espíndola (1999). "Evolution of the seismic activity from the 1982 eruption of El Chichón Volcano, Chiapas, Mexico". *Bulletin of Volcanology* 61(6), pages 411–422. DOI: 10.1007/s004450050282.

Laurent, A., C. Satriano, P. Bernard, N. Feuillet, and S. Jorry (2020). "Detection, location and characterization of VLF events during the 2018-2020 seismovolcanic crisis in Mayotte". *AGU Fall Meeting Abstracts*. Volume 2020, V040-0004, pages V040–0004.

Lavayssière, A., W. C. Crawford, J.-M. Saurel, C. Satriano, N. Feuillet, E. Jacques, and J.-C. Komorowski (2022). "A new 1D velocity model and absolute locations image the Mayotte seismo-volcanic region". *Journal of Volcanology and Geothermal Research* 421, page 107440. DOI: 10.1016/j.jvolgeores.2021.107440.

Lemoine, A., P. Briole, D. Bertil, A. Roullé, M. Foumelis, I. Thinon, D. Raucoules, M. de Michele, P. Valty, and R. Hoste Colomer (2020). "The 2018–2019 seismo-volcanic crisis east of Mayotte, Comoros islands: seismicity and ground deformation markers of an exceptional submarine eruption". *Geophysical Journal International* 223(1), pages 22–44. DOI: 10.1093/gji/ggaa273.

Lengliné, O., D. Marsan, J.-L. Got, V. Pinel, V. Ferrazzini, and P. G. Okubo (2008). "Seismicity and deformation induced by magma accumulation at three basaltic volcanoes". *Journal of Geophysical Research: Solid Earth* 113(B12). DOI: 10.1029/2008JB005937.

Lomax, A., J. Virieux, P. Volant, and C. Berge-Thierry (2000). "Probabilistic earthquake location in 3D and layered models". *Advances in seismic event location*. Edited by C. H. Thurber and N. Rabinowitz. Springer, pages 101–134.

Matoza, R. S., P. G. Okubo, and P. M. Shearer (2021). "Comprehensive High-Precision Relocation of Seismicity on the Island of Hawai'i 1986–2018". *Earth and Space Science* 8(1), pages 1–10. DOI: 10.1029/2020EA001253.

McKenzie, D., J. Jackson, and K. Priestley (2005). "Thermal structure of oceanic and continental lithosphere". *Earth and Planetary Science Letters* 233(3), pages 337–349. DOI: 10.1016/j.epsl.2005.02.005.

McNutt, S. R. and D. C. Roman (2015). "Volcanic Seismicity". *The Encyclopedia of Volcanoes*. Edited by H. B. T. Sigurdsson. 2nd edition. Amsterdam: Academic Press, pages 1011–1034. ISBN: 978-0-12-385938-9. DOI: 10.1016/B978-0-12-385938-9.00059-6.

Michon, L., V. Ferrazzini, A. Di Muro, N. Villeneuve, and V. Famin (2015). "Rift zones and magma plumbing system of Piton de la Fournaise volcano: How do they differ from Hawaii and Etna?" *Journal of Volcanology and Geothermal Research* 303, pages 112–129. DOI: 10.1016/j.jvolgeores.2015.07.031.

Mittal, T., J. S. Jordan, L. Retailleau, F. Beauducel, and A. Peltier (2022). "Mayotte 2018 eruption likely sourced from a magmatic mush". *Earth and Planetary Science Letters* 590, page 117566. DOI: 10.1016/j.epsl.2022.117566.

Morales-Yáñez, C., Z. Duputel, and L. Rivera (2022). "Exploring the link between large earthquakes and magma transport at the onset of the Mayotte volcano-seismic crisis". *Comptes Rendus. Géoscience* 354(S2), pages 137–152. DOI: 10.5802/crgeos.150.

Ortega-Romo, A. D. and X. Chen (2021). "Spatiotemporal clustering of seismicity during the 2018 Kilauea volcanic eruption". *Geophysical Research Letters* 48(8), e2020GL090859. DOI: 10.1029/2020GL090859.

Peltier, A., V. Ferrazzini, A. Di Muro, P. Kowalski, N. Villeneuve, N. Richter, O. Chevrel, J. L. Froger, A. Hrysiewicz, and M. Gouhier (2021). "Volcano crisis management at Piton de la Fournaise (La Réunion) during the COVID-19 lockdown". *Seismological Society of America* 92(1), pages 38–52. DOI: 10.1785/0220200212.

Peltier, A., S. Saur, V. Ballu, F. Beauducel, P. Briole, K. Chanard, D. Dausse, J.-B. de Chabalier, R. Grandin, P. Rouffiac, and Y.-T. Tranchant (2022). "Ground deformation monitoring of the eruption offshore Mayotte". *Comptes Rendus. Géoscience* 354(S2), pages 171–193. DOI: 10.5802/crgeos.176.

Power, J. A., M. M. Haney, S. M. Botnick, J. P. Dixon, D. Fee, A. M. Kaufman, D. M. Ketner, J. J. Lyons, T. Parker, J. F. Paskievitch, C. W. Read, C. Searcy, S. D. Stihler, G. Tepp, and A. G. Wech (2020). "Goals and Development of the Alaska Volcano Observatory Seismic Network and Application to Forecasting and Detecting Volcanic Eruptions". *Seismological Research Letters* 91(2A), pages 647–659. DOI: 10.1785/0220190216.

Ratdomopurbo, A. and G. Poupinet (2000). "An overview of the seismicity of Merapi volcano (Java, Indonesia), 1983-1994". *Journal of Volcanology and Geothermal Research* 100(1-4), pages 193–214. DOI: 10.1016/S0377-0273(00)00137-2.

Réseau de surveillance volcanologique et sismologique de Mayotte (REVOSIMA) (2022). "Bulletin de l'activité sismo-volcanique à Mayotte". http://www.ipgp.fr/fr/revosima.

Réseau Sismologique et géodésique Français (RÉSIF) (1995). "RESIF-RAP French Accelerometric Network". DOI: 10.15778/resif.ra.

Retailleau, L., J.-M. Saurel, M. Laporte, A. Lavayssière, V. Ferrazzini, W. Zhu, G. C. Beroza, C. Satriano, J.-C. Komorowski, and O. Team (2022). "Automatic detection for a comprehensive view of Mayotte seismicity". *Comptes Rendus. Géoscience* 354(S2), pages 1–18. DOI: 10.5802/crgeos.133.

Rinnert, E., N. Feuillet, Y. Fouquet, S. Jorry, I. Thinon, and E. Lebas (2019). *MAYOBS*. DOI: 10.18142/291.

Roman, D. C., S. De Angelis, J. L. Latchman, and R. White (2008). "Patterns of volcanotectonic seismicity and stress during the ongoing eruption of the Soufrière Hills Volcano, Montserrat (1995-2007)". *Journal of Volcanology and Geothermal Research* 173(3-4), pages 230–244. DOI: 10.1016/j.jvolgeores.2008.01.014.

Roman, D. C. and K. V. Cashman (2018). "Top–down precursory volcanic seismicity: implications for 'stealth' magma ascent and long-term eruption forecasting". *Frontiers in Earth Science* 6, page 124. DOI: 10.3389/feart.2018.00124.

Saurel, J.-M., E. Jacques, C. Aiken, A. Lemoine, L. Retailleau, A. Lavayssière, O. Foix, A. Dofal, A. Laurent, N. Mercury, W. Crawford, A. Lemarchand, R. Daniel, P. Pelleau, M. Bès de Berc, G. Dectot, D. Bertil, A. Roullé, C. Broucke, A. Colombain, H. Jund, S. Besançon, P. Guyavarch, P. Kowalski, M. Roudaut, R. Appriou, J. Battaglia, S. Bodihar, P. Boissier, M. P. Bouin, C. Brunet, K. Canjamale, P. Catherine, N. Desfete, C. Doubre, R. Dretzen, T. Dumouche, P. Fernagu, V. Ferrazzini, F. R. Fontaine, A. Gaillot, L. Géli, C. Griot, M. Grunberg, E. C. Guzel, R. Hoste-Colomer, S. Lambotte, F. Lauret, F. Léger, E. Maros, A. Peltier, J. Vergne, C. Satriano, F. Tronel, J. Van der Woerd, Y. Fouquet, S. J. Jorry, E. Rinnert, I. Thinon, and N. Feuillet (2022). "Mayotte seismic crisis: building knowledge in near real-time by combining land and ocean-bottom seismometers, first results". *Geophysical Journal International* 228(2), pages 1281–1293. DOI: 10.1093/gji/ggab392.

Shapiro, N. M., D. V. Droznin, S. Y. Droznina, S. L. Senyukov, A. A. Gusev, and E. I. Gordeev (2017). "Deep and shallow long-period volcanic seismicity linked by fluid-pressure transfer". *Nature Geoscience* 10(6), pages 442–445. DOI: 10.1038/ngeo2952.

Tait, S., C. Jaupart, and S. Vergniolle (1989). "Pressure, gas content and eruption periodicity of a shallow, crystallising magma chamber". *Earth and Planetary Science Letters* 92(1), pages 107–123. DOI: 10.1016/0012-821X(89)90025-3.

Wessel, P., J. F. Luis, L. Uieda, R. Scharroo, F. Wobbe, W. H. F. Smith, and D. Tian (2019). "The Generic Mapping Tools Version 6". *Geochemistry, Geophysics, Geosystems* 20(11), pages 5556–5564. DOI: 10.1029/2019GC008515.

Wilding, J. D., W. Zhu, Z. E. Ross, and J. M. Jackson (2022). "The magmatic web beneath Hawai'i". *Science* 379(6631), pages 462–468. DOI: 10.1126/science.ade5755.

Wright, T. L. and F. W. Klein (2006). "Deep magma transport at Kilauea volcano, Hawaii". *Lithos* 87(1), pages 50–79. DOI: 10.1016/j.lithos.2005.05.004.

Zhu, W. and G. C. Beroza (2019). "PhaseNet: a deep-neural-network-based seismic arrival-time picking method". *Geophysical Journal International* 216(1), pages 261–273. DOI: 10.1093/gji/ggy423.